Interactive CardioVascular and Thoracic Surgery 30 (2020) 879–886
doi:10.1093/icvts/ivaa037 Advance Access publication 4 April 2020

ORIGINAL ARTICLE

Cite this article as: Xuan Y, Dvir D, Wang Z, Ye J, Guccione JM, Ge L *et al.* Stent and leaflet stresses across generations of balloon-expandable transcatheter aortic valves. Interact CardioVasc Thorac Surg 2020;30:879–86.

Stent and leaflet stresses across generations of balloon-expandable transcatheter aortic valves

Yue Xuan[a], Danny Dvir[b], Zhongjie Wang[a], Jian Ye[c], Julius M. Guccione[a], Liang Ge[a] and Elaine E. Tseng[a,*]

[a] Division of Cardiothoracic Surgery, University of California San Francisco and San Francisco VA Medical Center, San Francisco, CA, USA
[b] Division of Cardiology, University of Washington, Seattle, WA, USA
[c] Department of Surgery, St Paul's Hospital, Vancouver, BC, Canada

* Corresponding author. Division of Cardiothoracic Surgery, University of California San Francisco and San Francisco VA Medical Center, 500 Parnassus Ave., Suite 405W, Box 0118, San Francisco, CA 94143-0118, USA. Tel: +1-415-2214810/x23452; fax: +1-415-7502181; e-mail: elaine.tseng@ucsf.edu (E.E. Tseng).

Received 19 June 2019; received in revised form 10 January 2020; accepted 4 February 2020

ADULT CARDIAC

Key question

What leaflet stresses on balloon-expandable SAPIEN transcatheter heart valves across generations may affect long-term durability?

Key finding(s)

Maximum stresses in similar leaflet locations across generations. SAPIEN 3 had the highest stresses in 26-mm and 29-mm sizes.

Take-home message

Latest generation SAPIEN 3 had highest stresses in larger sizes. High leaflet stresses may be associated with early degeneration.

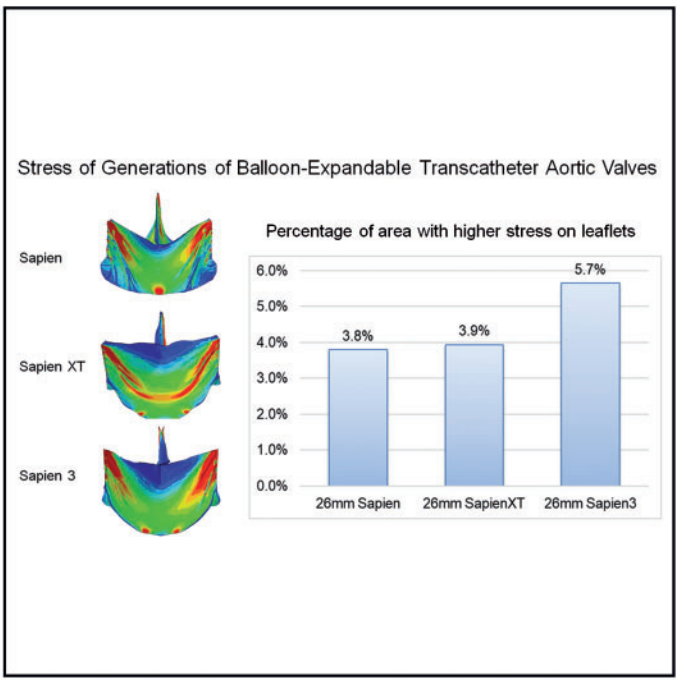

Abstract

OBJECTIVES: Transcatheter aortic valve replacement (TAVR) is established therapy for severe aortic stenosis patients with intermediate-, high- and prohibitive-risk for surgery. A significant challenge when expanding TAVR to low-risk and younger patients is the unknown long-term durability. High leaflet stresses have been associated with surgical bioprosthetic valve degeneration. In this study, we examined the impact of changes in valve design across 3 generations of same-sized TAVR devices on stent and leaflet stresses.

METHODS: The 26-mm Edwards SAPIEN, 23, 26 and 29 mm SAPIEN XT (XT) and 26 mm SAPIEN 3 (S3) ($n = 1$ each) underwent micro-computed tomography (micro-CT) scanning. Dynamic finite element computational simulations of 23–26 mm SAPIEN, 23–29 mm XT and 23–29 mm S3 were performed with physiological loading and micro-CT or scaled geometries.

RESULTS: Peak stresses were concentrated in the commissure area and along the bottom of the suture, representing areas most likely to develop structural valve degeneration across TAVR generations. Latest-generation S3 showed greatest 99th percentile principal stress on commissural leaflets for 26 and 29 mm, and increased stresses over XT for 23 mm. Percentage of higher stress areas within the

Presented at EuroPCR the annual meeting of the European Association of Percutaneous Cardiovascular Interventions, Paris, France, 16–19 May 2017.

leaflets steadily increased across generations, 3.8%, 3.9% and 5.7%, respectively, for 26 mm SAPIEN, XT and S3 with similar trend for 29-mm valves.

CONCLUSIONS: Using computational simulations based on high-fidelity modelling of balloon-expandable TAVRs, our study demonstrated that maximum stress areas existed in similar leaflet locations across SAPIEN generations, while the latest model S3 had the highest magnitude for both 26- and 29-mm valves. S3 also had the largest area of higher stresses than other generations, which would be prone to degeneration. Our study coupled with future long-term clinical outcomes >10 years will provide insight on biomechanics of TAVR degeneration.

Keywords: Transcatheter heart valve • Balloon expandable • Computational simulation • Durability

ABBREVIATIONS

micro-CT	Micro-computed tomography
S3	SAPIEN 3
SAVR	Surgical aortic valve replacement
SVD	Structural valve degeneration
TAVR	Transcatheter aortic valve replacement
THV	Transcatheter heart valve
XT	SAPIEN XT

INTRODUCTION

Transcatheter aortic valve replacement (TAVR) is established as the standard of care for inoperable, high- and intermediate-risk patients with severe symptomatic aortic stenosis [1–3]. In recent randomized clinical trials of low-risk aortic stenosis patients, self-expanding TAVR demonstrated non-inferiority to surgical aortic valve replacement (SAVR) at 2 years, while balloon-expandable TAVR showed superiority to SAVR with respect to composite outcomes of death, stroke, and rehospitalization at 1 year [4, 5]. With such excellent clinical outcomes, TAVR will expand to low-risk patients who typically are younger; yet, TAVR durability is unknown. Follow-up of these clinical trials for TAVR versus SAVR durability will require a minimum of 15 years.

In the meantime, from a biomechanical perspective, valve design influences durability [6]; and high stress levels on valve leaflets have been demonstrated to be associated with early degeneration of surgical bioprostheses [7–9]. Leaflet stresses, which cannot be measured clinically, may be determined using advanced computational simulations. We have previously performed computational studies of selected transcatheter heart valve (THV) designs and sizes to determine THV leaflet stresses under quasi-static loading [10–12]. The objective of the current study was to quantify and compare stresses on 3 generations of balloon-expandable THVs under dynamic physiological loading conditions to understand the iterative influence of changes in valve design. Our results lay the foundation for a biomechanical understanding of long-term TAVR durability.

MATERIALS AND METHODS

In order to develop a computational model to accurately compare stress, precise three-dimensional geometry in a zero-stress state, material properties of each component, boundary conditions and physiological loading conditions in finite element simulation are required.

Transcatheter heart valve geometry

Eight total THVs of 3 sizes were simulated for the current study—23 and 26 mm SAPIEN; 23, 26 and 29 mm SAPIEN XT (XT); and 23, 26 and 29 mm SAPIEN 3 (S3). We previously described the method of THV geometry development [10–12]. In brief, commercial 26 mm SAPIEN, XT and S3 ($n = 1$ each) and 23 and 29 mm XT ($n = 1$ each) THVs (Edwards Lifesciences, Inc., Irvine, CA, USA) (Table 1) underwent micro-computed tomography (micro-CT) scanning in different orientations and settings to distinguish stent and leaflet geometries. High-resolution radiological images were manually segmented to obtain the most accurate representation of stent and leaflets. Reconstructed geometries were then refined to generate the precise geometry of the fully expanded THV assembly, consisting of stent, Dacron covering, suture and bovine pericardial leaflets. S3 had an additional external skirt around the stent bottom. Geometry of the 26 mm SAPIEN, XT and S3, and the 23 and 29 mm XT was reconstructed based on micro-CT scans, while the geometry of 23 mm SAPIEN was scaled from 26 mm SAPIEN, and 23 and 29 mm S3 were scaled from the 26 mm S3.

Finite element analysis

Geometry of leaflets and Dacron was then meshed into shell elements, while the stent was meshed into hexahedral solid elements. Mesh convergence studies were performed to optimize the mesh size. Based on the convergence studies, the element sizes were selected and total number of elements listed in Table 1 (Fig. 1A). Suture connections between different components were simulated to enable accurate representation of the assembly between leaflet and stent, leaflet and Dacron and Dacron and stent [10–12].

Finite element simulation of each THV under dynamic physiological loading of systemic pressure was implemented in ABAQUS solver (Dassault Systemes, Waltham, MA, USA). Material properties of THV leaflets [13] and the constitutive material model have been described in previous studies [10–12]. The leaflet thickness was measured using a digital calibre. The thinnest thickness measured from each valve was 0.24 mm. For each valve model, the leaflet thickness was then set to 0.24 mm. The current study thus corresponds to the highest leaflet stress potential for each valve design. Contact between each pair of contact components was defined to most closely represent the contact interaction behaviour [10–12]. Leaflets and stent were loaded to physiological cycles of systemic pressures in the fully expanded configuration. After initial pressurization, cardiac cycles of 800-ms duration were applied and stresses were computed for each THV.

Table 1: Characteristics of 3 generations of SAPIEN valves

	SAPIEN	SAPIEN XT	SAPIEN 3
Leaflet thickness averaged (min–max) (mm)	0.32 (0.24–0.36)	0.32 (0.24–0.37)	0.26 (0.24–0.26)
Leaflet surface area (mm^2)	756–965	775–1236	883–1414
Leaflet curvature[a] (/mm)	0.19–0.22	0.15–0.29	0.19–0.34
Commissure connection	Radial stent	Radial stent	Circumferential stent
Stent material	Stainless steel	Cobalt-chromium	Cobalt-chromium
Stent design	4 layers	3 layers	5 layers
Leaflet element number	21 510	20 988	20 988
Stent element number	5892	6336	6168

[a]Leaflet curvature is the reciprocal of the radius *R*.

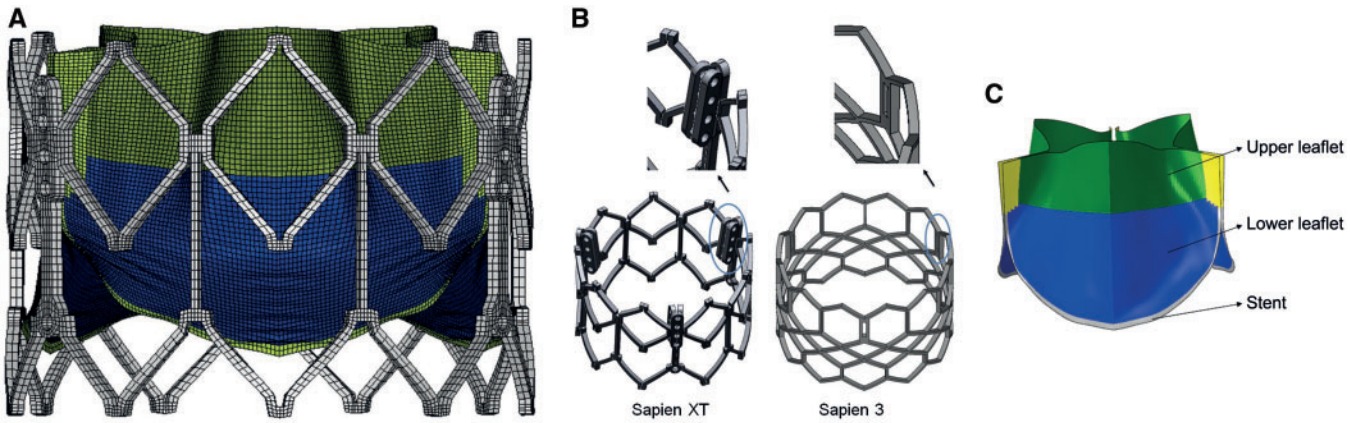

Figure 1: (**A**) Representative mesh of 26 mm SAPIEN XT; (**B**) commissure-stent attachment of SAPIEN and SAPIEN XT versus SAPIEN 3; and (**C**) subregions of balloon-expandable transcatheter heart valve leaflet.

Statistical analysis

Statistical analysis was performed using R (R 3.5.1). Wilcoxon Rank-Sum test was used to compare peak stresses of different SAPIEN generations. A 2-sided *P*-value <0.05 was considered statistically significant. The 99th percentile stresses [14] were reported and used for statistical analysis. The 99th percentile stresses have previously been demonstrated more reproducible than maximum stresses because it avoids non-physiological peak stresses that can occur due to inhomogeneities in the mesh. For simplicity, maximum principal stresses will hereafter indicate the 99th percentile principal stresses. A repeatability study was carried out by 2 independent investigators for a subset of all XT sizes and the variation of the peak stress was within 5%. Details of the repeatability study can be found in our previous study [15].

RESULTS

Maximum principal stresses (tension forces) and minimum principal stresses (compression forces), location and magnitude of peak principal stresses at diastolic pressure (80 mmHg) are reported. Maximum principal stress values correspond to tensile stress where THV leaflets stretch to the closed configuration, while minimum principal stresses represent leaflet bending where redundant tissue is compressed. For 26-mm THV leaflets, maximum principal stresses across the entire leaflet, including sutured regions, were 1.61, 1.36 and 1.63 MPa, respectively, for SAPIEN, XT and S3 at 80 mmHg (Fig. 2A–C). Minimum principal stresses across the entire leaflet were -0.25, -0.15 and -0.15 MPa for SAPIEN, XT and S3, respectively (Fig 2D–F). Maximum and minimum principal stresses for each subregion are listed (Table 2). The sutured edges held the maximum and minimum principal stresses for the entire leaflet assembly in each THV generation. Peak stresses occurred at tips of leaflet commissures attached to the stent in S3 (Fig. 1B) and occurred at the bottom suture of leaflets in SAPIEN and XT. Stresses at the commissure area of SAPIEN and XT were attenuated by leaflet attachment to the radial bar. In contrast, regions of free leaflet margin at the top and leaflet belly had relatively lower peak stresses.

In addition to magnitude of peak stresses, the areas of high stress concentration were also determined. High stress levels were defined as stress level over the cut-off value of mean plus 1.75 times of the standard deviation of total leaflet stresses. Percentages of high-stress areas on the leaflets were 3.8%, 3.9% and 5.7% for 26 mm SAPIEN, XT and S3, respectively. Mean leaflet stresses were 0.31 ± 0.22 MPa for all 26-mm THV models. The 26-mm THV stress distributions were significantly different between SAPIEN and XT ($P < 0.0001$), SAPIEN and S3 ($P < 0.0001$) and XT and S3 ($P < 0.0001$). A histogram of stress distribution on the leaflets for each THV of the 3 generations is shown (Fig. 3).

Similarly, the stress distribution on 23- and 29-mm THV leaflets across generations showed a similar trend to the 26-mm THVs. For the 29-mm THV, peak leaflet stresses were 1.88 MPa for S3 versus 1.02 MPa for XT. SAPIEN was only created with 23 and 26 mm sizes and did not have a 29 mm size. For the 23-mm THVs, peak leaflet stresses increased from XT to S3, 1.21 MPa on S3 and 1.11 MPa on XT, but was highest 1.47 MPa on SAPIEN.

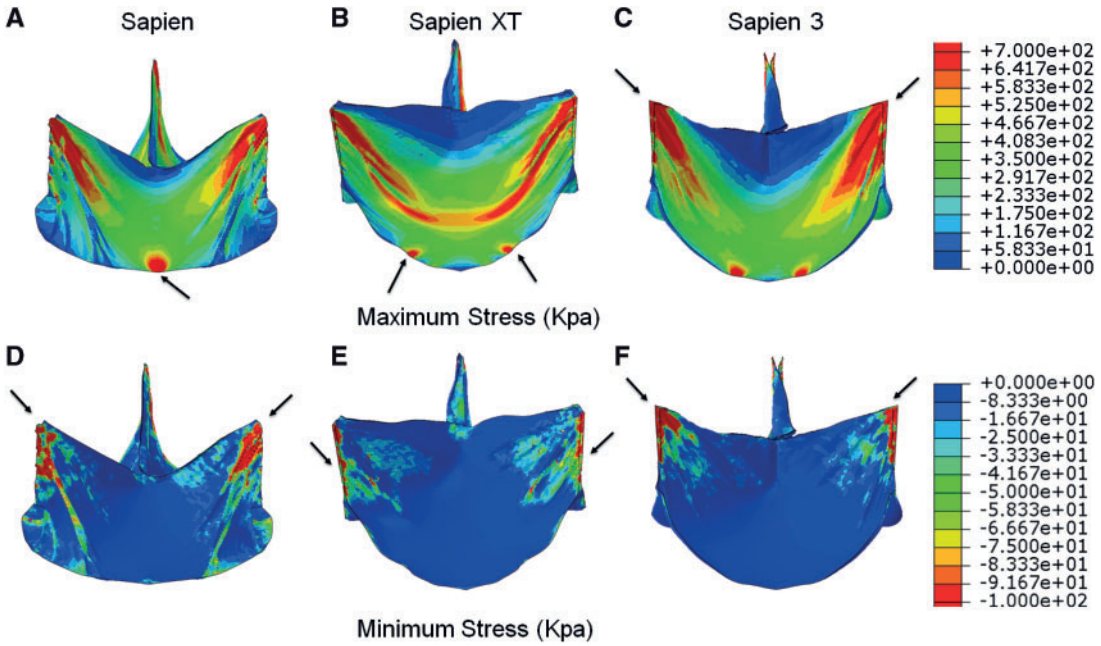

Figure 2: Maximum principal stresses on leaflets of 26 mm (**A**) SAPIEN, (**B**) SAPIEN XT and (**C**) SAPIEN 3 and minimum principal stresses on leaflets of 26 mm (**D**) SAPIEN, (**E**) SAPIEN XT and (**F**) SAPIEN 3. Arrow indicates the location of the maximum or minimum stress.

Table 2: Maximum and minimum principal stresses on leaflet regions with closed configuration

	Max principal stress 99th percentile (MPa)			Min principal stress 99th percentile (MPa)		
	SAPIEN	XT	S3	SAPIEN	XT	S3
26 mm						
Upper leaflet	0.98	0.88	1.63	-0.29	-0.06	-0.15
Lower leaflet	0.74	0.82	0.73	-0.1	-0.07	-0.04
Suture	1.61	1.36	1.22	-0.09	-0.15	-0.08
Stent	42.05	29.19	24.34	-44.5	-31.17	-25.94
23 mm						
Upper leaflet	0.91	1.11	1.21	-0.27	-0.08	-0.1
Lower leaflet	0.64	0.46	0.68	-0.09	-0.05	-0.04
Suture	1.47	0.88	1.06	-0.1	-0.18	-0.06
Stent	42.40	30.51	23.79	-45.29	-29.64	-25.55
29 mm						
Upper leaflet		1.02	1.88		-0.08	-0.16
Lower leaflet		0.58	0.81		-0.05	-0.06
Suture		1.02	1.56		-0.12	-0.08
Stent		28.77	24.24		-30.25	-25.87

S3: SAPIEN 3; XT: SAPIEN XT.

Histograms of the stress distribution demonstrated a similar trend as the 26-mm THVs. The 29-mm S3 had the largest percentage of leaflet area with higher stress levels (7.9%), while both 23 mm XT and 23 mm S3 had larger percentage of leaflet area with higher stress levels (3.7% and 3.8%).

For the 26-mm stent, maximum principal stresses at diastolic pressure were 42.05, 29.19 and 24.34 MPa on SAPIEN, XT and S3, respectively. Minimum principal stresses at diastolic pressure were -44.5, -31.17 and -25.94 MPa on SAPIEN, XT and S3, respectively (Fig. 4). Peak stresses on the stent occurred close to where the THV was deployed and constrained above the annulus and also occurred on the distal struts. For the 23-mm THVs, maximum principal stresses at diastolic pressure were 42.40, 30.51 and 23.79 MPa and minimum principal stresses at diastolic pressure were -45.29, -29.64 and -25.55 MPa on SAPIEN, XT and S3, respectively. Similarly, for the 29-mm THV, maximum principal stresses at diastolic pressure were 28.77 and 24.24 MPa and minimum principal stresses at diastolic pressure were -30.25 and -25.87 MPa on XT and S3, respectively.

DISCUSSION

In this study, we examined leaflet stresses across 3 generations of balloon-expandable SAPIEN THV devices through computational simulation as a surrogate to compare long-term durability based upon valve design. We found that with valve design iterations, the latest third-generation S3 in general had the highest peak stresses for 26- and 29-mm THVs and the largest area of higher stresses for 26- and 29-mm THVs compared to the prior 2

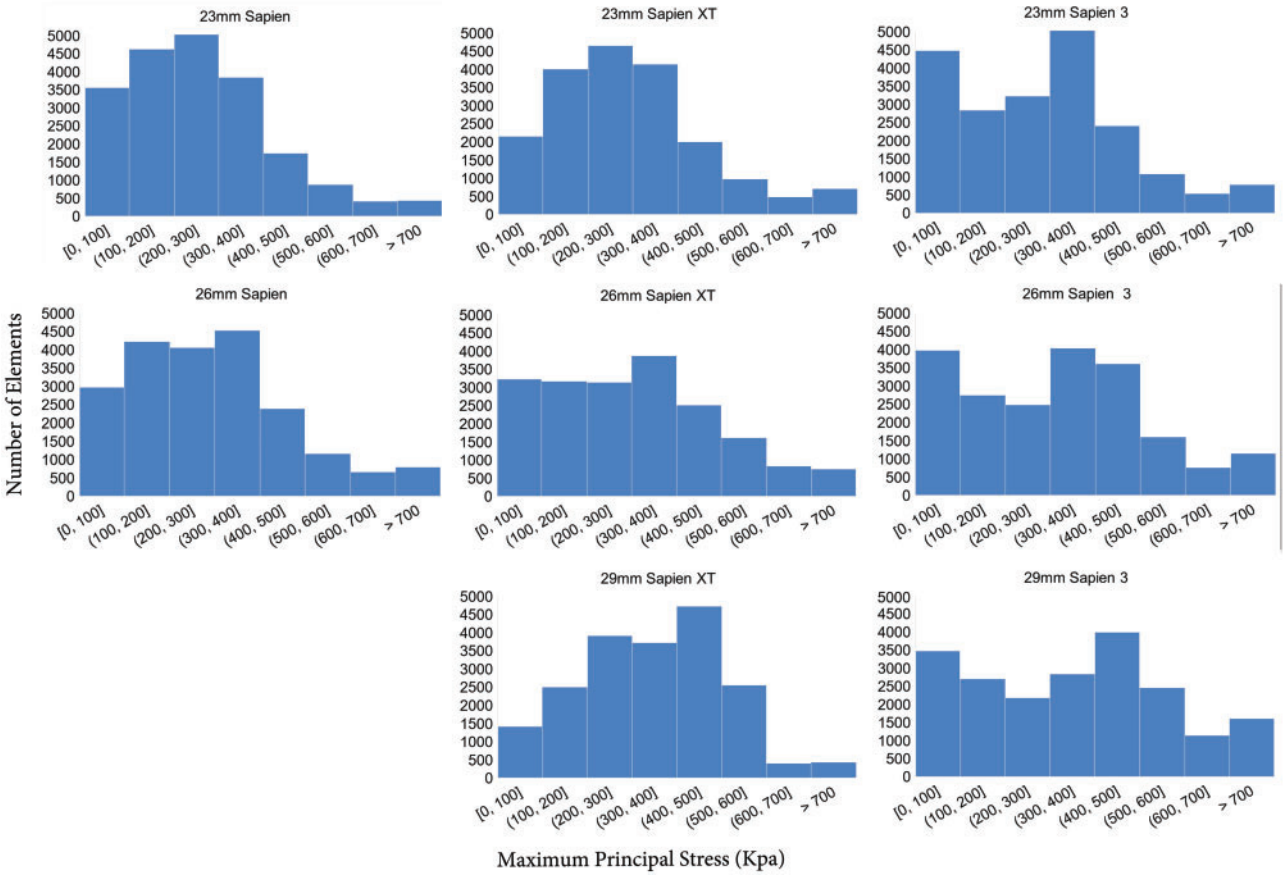

Figure 3: Histogram of maximum stress on leaflets of 23, 26 and 29 mm SAPIEN, SAPIEN XT and SAPIEN 3.

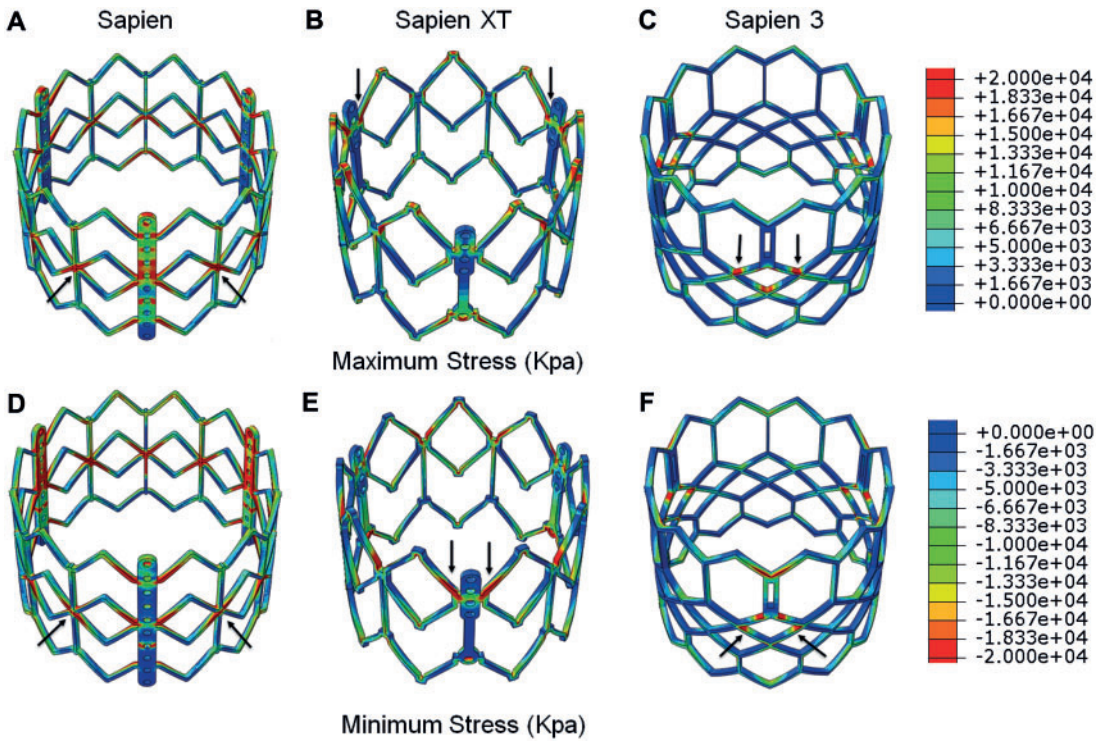

Figure 4: Maximum principal stresses on stent of 26 mm (**A**) SAPIEN, (**B**) SAPIEN XT and (**C**) SAPIEN 3 and minimum principal stresses on stent of 26 mm (**D**) SAPIEN, (**E**) SAPIEN XT and (**F**) SAPIEN 3. Arrow indicates the location of the maximum or minimum stress.

generations. The 23-mm first-generation SAPIEN had the highest stresses compared to both second and third generations, while both 23 mm XT and S3 had the largest area of higher stresses. These areas of higher peak stresses would be subject to early structural valve degeneration (SVD). Clinical degeneration data as they become available combined with our analysis will improve our biomechanical understanding of long-term THV durability.

Structural valve degeneration

SVD is a complex process impacted by multiple factors, in addition to leaflet stresses, such as deployed patient-specific geometry, younger patient age and prosthesis–patient mismatch [6–9, 16, 17]. SVD of bioprosthetic valves presents as thickening, calcification and tearing of the valve, or disruption of valve microstructure resulting in stenosis or regurgitation [6, 7, 17]. Since SAPIEN was approved in USA in 2011, US patients received SAPIEN, then XT, and more recently, S3. Five-year outcomes of PARTNER trial revealed no SVD with maintenance of low gradients and increased valve area [1, 2]. While short-term outcomes have significantly improved with iterative generations of SAPIEN, questions remain regarding long-term durability as TAVR expands to younger intermediate- and low-risk patients. Despite the first TAVR in 2002, little data exist for long-term outcomes >10 years because of the advanced age of patients (average 80 years old) in the original randomized trials. Vast majority of these elderly patients died within 5 years of TAVR and hence too few remaining patients were alive >5 years to appropriately comment on durability [18]. In contrast, a long-term study of Carpentier-Edwards Perimount pericardial surgical bioprosthesis implanted between 1984 and 2008 showed actuarial freedom from SVD at 10, 15 and 20 years of 94%, 79% and 49%, respectively [19].

Increased leaflet stresses, among clinical risk factors, may initiate and accelerate SVD, and have been shown to correlate with calcific degeneration, thickening or leaflet tearing [6, 9, 17]. Generally, the higher stresses concentrated on the commissure suture and bottom suture area for all 3 generations of THVs. Those areas may be highly prone to SVD—calcification, thickening or tearing. Early evidence showed that the location of calcification in surgical bioprosthetic aortic valves was along the bottom edge and commissure areas [20]. With future clinical evidence of THV SVD, we can better understand the effect of mechanical stress on SVD. Collagen fibre fixation, a standard pretreatment process for all bioprostheses, prevented normal structural internal rearrangements, causing increased tissue rigidity and greater mechanical stresses during opening and closing compared to native valve leaflets. Design-related mechanical stresses were identified as important causes of SVD [6, 7, 16, 17]. On the one hand, areas of calcification correlated to areas of high mechanical stresses in bioprostheses. On the other hand, tearing and rupture of leaflets were often spatially distributed in areas of calcium deposition. Tearing occurred at locations of increased mechanical deformations during leaflet motion. Thus, understanding THV leaflet stresses is the first step towards understanding THV long-term durability.

Valve design and stress

Previous studies of Edwards 25-mm Perimount surgical bioprostheses found leaflet stresses ranging from 544.7 to 663.2 kPa at 120 mmHg under quasi-static conditions [7]. The elevated stress levels of all THV leaflets seen here in comparison are in part due to the reduced thickness of the leaflet. For S3, peak stresses were on the commissure suture, which was affected by the stent design as shown in Fig. 1B. TAVR devices rapidly developed over the past decade with each subsequent generation designed to facilitate technical implantation and to optimize procedural outcomes. SAPIEN THVs were designed with bovine pericardium treated by the same anti-calcification processes as the surgical Carpentier-Edwards aortic pericardial valves [10–12]. THV leaflets were processed to be thinner, approximately half that of surgical bioprostheses (Table 1) [13] to facilitate reduction in profile of the XT and S3 delivery systems. We found overall leaflet stresses with SAPIEN THVs increased based upon reduced leaflet thickness and valve design changes across generations and compared to surgical bioprostheses [7]. XT modified SAPIEN's fully open leaflet design to semi-closed leaflet to reduce complications of intravalvular leakage from leaflets stuck in the open position. As such, SAPIEN leaflets are less curved and flatter along the annulus and suture line to the stent (Fig. 2), whereas XT leaflets are more curved and U shaped as they attach to the Dacron and stent. Third-generation S3 added an outer sealing skirt to reduce paravalvular leakage. S3 leaflets are similar in shape to those of XT, but S3 are sutured to the circumferential stent rather than sutured through a radial bar to the stent in SAPIEN and XT (Fig. 1B). This change maximized effective orifice area and allowed more radial flexibility of the leaflets with extended free edges, but led to increased stresses on the commissures of S3 compared to SAPIEN and XT, where maximum principal stresses were along the leaflet bottom. The leaflets' free edges where the 3 leaflets coapted had low stress magnitude. Low stress reflected minimum pressure and deformation in this area in the closed configuration. S3 had the largest area of low stress distribution in the coaptation area due to its leaflet shape and curvature, and thus calcification would be less likely at the free edge.

Stress differences found on the THV stent across generations were caused by different stent materials and frame design. First-generation SAPIEN stent was made of stainless steel with diamond-shaped open cell lattices and uniform layout in the circumferential and longitudinal directions. Six struts 120° apart were aligned along the radial direction towards the centre. Subsequently, the delivery systems were developed with smaller profiles, and SAPIEN was superseded by low-profile XT, with a cobalt-chromium alloy frame, which allowed a thinner, stronger and compressible frame with more open strut structure than its predecessor. XT open cell lattices were large with 3 layers of repeated pattern instead of 4 in SAPIEN. S3 stent has larger and fewer open cell lattices allowing further size reduction of delivery system to 14 Fr for transfemoral implantation with the same cobalt-chromium material. S3 has non-uniform open cell lattice with much larger openings distally to allow for easy access for percutaneous coronary intervention.

Prior THV computational simulations showed similar magnitudes of THV leaflet stresses as our study [21–23]. When comparing our study to earlier computational studies, variations in THV leaflet stresses are largely accounted for by differences in material properties, generic versus precise geometry, THV diameter and leaflet thickness. Early computational simulations on THV leaflets lacked precise three-dimensional geometry of the commercial THV leaflets sutured to the stent compared to our study. Average leaflet stresses on a generic 23-mm-diameter THV were 1.56 MPa with peak of 2.52 MPa [21]. Furthermore, leaflet stresses were also impacted by quasi-static versus physiological dynamic blood

pressure loading conditions. Notably, our prior THV simulations of different-sized THVs reported peak [10–12] rather than 99% peak leaflet stresses. Also, the current study is dynamic simulations which could yield higher peak stresses than quasi-static loading in our previous studies. Estimated TAVR durability was also highly dependent on leaflet thickness. Leaflet stresses decreased with increasing tissue thickness during simulations of thin pericardial THV bioprosthetic valve leaflet deformation under static pressure-only loading conditions [22]. Previous studies also showed both THV undersizing [22] and oversizing [11], and irregular deployment [12] resulted in stress variations along different regions of the bioprosthetic valve. However, no prior study examined the influence of valve design across THV generations on leaflet stresses using a consistent THV nominal size to understand baseline differences in leaflet stresses prior to patient-specific deployment as we have demonstrated here.

In addition, a fatigue simulation of bioprosthetic heart valve suggested that TAVR durability is expected to be 7.8 years [23]. The SAVR failure point was 28N and they assumed that SAVR had a durability of 20 years. Thus, for TAVR, with a 9N state representing 82% of the fatigue life, the expected durability of THVs was proportionally scaled to be 7.8 years. For both valves in their simulation, peak leaflet damages were predicted near the commissures and along the stent attachments which is consistent with the peak stress region in our study.

As we await long-term 10- to 15-year THV clinical outcomes in <80-year-old patients, finite element studies which examine leaflet stresses in generations of THV designs provide critical information to understand the impact of THV design changes on long-term durability. In this study, we demonstrated that design improvements to facilitate clinical implantation, i.e. changes in design to allow reduced THV profile, also had effects on stent and leaflet stresses such that the latest-generation S3 had the highest leaflet stress compared to earlier generations in 26- and 29-mm THVs.

Limitations

Our study did not take into account the process of crimping and ballooning, as THV geometry after deployment is variable and understanding the impact of THV design changes across generations required consistent manufactured geometry. The crimping and ballooning process leads to plastic deformation on the stent. Such plastic deformation was not modelled in our current work and will be addressed in the future. Crimping physically damages THV leaflets, which may weaken leaflets and increase leaflet stress [24]. We did not destroy our THVs to test their leaflets for exact material properties, given the rarity of obtaining THVs and need for future THV experimental *in vitro* tests. As such, we utilized excised leaflets from surgical bioprostheses to determine material properties for THV leaflets, but with leaflet thickness directly incorporated from THV. The thinness of THV leaflets accounts for its reduced strength and higher stresses. Notably, as the leaflet material properties remained constant among the 3 THV generations, we expect the trends seen in our results to be representative of those seen with THV leaflet material properties. As stent and leaflet stresses cannot be directly measured, our stress analyses cannot be experimentally validated. It is noted that the patient-specific configuration such as the calcified native valves and THV deployed shape could lead to non-trivial variation of the leaflet and stent stresses. The irregular configuration also can induce turbulence which is beyond the scope of the current study. Patient-specific THV deployment with calcified native valves will be included in future study. However, given that our purpose was to understand the impact of device design changes as THV generations evolved, patient-specific simulations would have presented as a confounder and clearer interpretation of design changes is reflected in this *ex vivo* study of nominal manufactured THVs. Lastly, we cannot comment on THV stress variation within generations due to limited THV supply, but anticipate that commercial manufacturing processes require strict adherence to reproducibility of valve production.

Funding

This work was funded by the University of California Proof of Concept [#246590], National Institutes of Health [R01HL119857] and American Heart Association postdoctoral fellowship [16POST31420013].

Conflict of interest: Elaine E. Tseng and Liang Ge are the founders of ReValve Med, Inc. Danny Dvir and Jian Ye report consulting fees from Edwards Lifesciences. All other authors declared no conflict of interest.

Author contributions

Yue Xuan: Conceptualization; Data curation; Formal analysis; Funding acquisition; Investigation; Methodology; Project administration; Resources; Software; Supervision; Validation; Visualization; Writing—original draft; Writing—review & editing. **Danny Dvir:** Conceptualization; Data curation; Formal analysis; Investigation; Methodology; Project administration; Resources; Software; Supervision; Validation; Visualization; Writing—original draft. **Zhongjie Wang:** Conceptualization; Data curation; Formal analysis; Investigation; Methodology; Project administration; Resources; Software; Validation; Visualization; Writing—original draft. **Jian Ye:** Conceptualization; Data curation; Formal analysis; Investigation; Methodology; Project administration; Resources; Software; Supervision; Validation; Visualization; Writing—original draft; Writing—review & editing. **Julius M. Guccione:** Conceptualization; Data curation; Formal analysis; Investigation; Methodology; Resources; Software; Supervision; Validation; Visualization; Writing—original draft; Writing—review & editing. **Liang Ge:** Conceptualization; Data curation; Formal analysis; Funding acquisition; Investigation; Methodology; Project administration; Resources; Software; Supervision; Validation; Writing—original draft; Writing—review & editing. **Elaine E. Tseng:** Conceptualization; Data curation; Formal analysis; Funding acquisition; Investigation; Methodology; Project administration; Resources; Software; Supervision; Validation; Visualization; Writing—original draft; Writing—review & editing.

REFERENCES

[1] Kapadia SR, Leon MB, Makkar RR, Tuzcu EM, Svensson LG, Kodali S *et al.* 5-Year outcomes of transcatheter aortic valve replacement compared with standard treatment for patients with inoperable aortic stenosis (partner 1): a randomised controlled trial. Lancet 2015;385:2485–91.

[2] Mack MJ, Leon MB, Smith CR, Miller DC, Moses JW, Tuzcu EM *et al.* 5-Year outcomes of transcatheter aortic valve replacement or surgical aortic valve replacement for high surgical risk patients with aortic stenosis (partner 1): a randomised controlled trial. Lancet 2015;385:2477–84.

[3] Reardon MJ, Van Mieghem NM, Popma JJ, Kleiman NS, Søndergaard L, Mumtaz M *et al.* Surgical or transcatheter aortic-valve replacement in intermediate-risk patients. N Engl J Med 2017;376:1321–31.

[4] Popma JJ, Deeb GM, Yakubov SJ, Mumtaz M, Gada H, O'Hair D *et al.* Transcatheter aortic-valve replacement with a self-expanding valve in low-risk patients. N Engl J Med 2019;380:1706–15.

[5] Mack MJ, Leon MB, Thourani VH, Makkar R, Kodali SK, Russo M *et al*. Transcatheter aortic-valve replacement with a balloon-expandable valve in low-risk patients. N Engl J Med 2019;380:1695–705.
[6] Thubrikar MJ, Deck JD, Aouad J, Nolan SP. Role of mechanical stress in calcification of aortic bioprosthetic valves. J Thorac Cardiovasc Surg 1983;86:115–25.
[7] Sun W, Abad A, Sacks MS. Simulated bioprosthetic heart valve deformation under quasi-static loading. J Biomech Eng 2005;127:905–14.
[8] Masters RG, Walley VM, Pipe AL, Keon WJ. Long-term experience with the Ionescu-Shiley pericardial valve. Ann Thorac Surg 1995;60(2 Suppl): S288–91.
[9] Sabbah HN, Hamid MS, Stein PD. Mechanical factors in the degeneration of porcine bioprosthetic valves: an overview. J Card Surg 1989;4: 302–9.
[10] Xuan Y, Dvir D, Wang Z, Mizoguchi T, Ye J, Guccione JM *et al*. Stent and leaflet stresses in 26-mm, third-generation, balloon-expandable transcatheter aortic valve. J Thorac Cardiovasc Surg 2019;157:528–36.
[11] Xuan Y, Krishnan K, Ye J, Dvir D, Guccione JM, Ge L *et al*. Stent and leaflet stresses in 29-mm second-generation balloon-expandable transcatheter aortic valve. Ann Thorac Surg 2017;104:773–81.
[12] Xuan Y, Krishnan K, Ye J, Dvir D, Guccione JM, Ge L *et al*. Stent and leaflet stresses in a 26-mm first-generation balloon-expandable transcatheter aortic valve. J Thorac Cardiovasc Surg 2017;153: 1065–73.
[13] Kuang H, Xuan Y, Lu M, Mookhoek A, Wisneski AD, Guccione JM *et al*. Leaflet mechanical properties of Carpentier-Edwards Perimount Magna pericardial aortic bioprostheses. J Heart Valve Dis 2017;26:81–9.
[14] Speelman L, Bosboom EM, Schurink GW, Hellenthal FA, Buth J, Breeuwer M *et al*. Patient-specific AAA wall stress analysis: 99-percentile versus peak stress. Eur J Vasc Endovasc Surg 2008;36:668–76.
[15] Xuan Y, Dvir D, Wisneski A, Wang Z, Ye J, Guccione J *et al*. Impact of transcatheter aortic valve size on leaflet stresses: implications for durability and optimal grey zone sizing. AsiaIntervention 2020; in press.
[16] Senage T, Le Tourneau T, Foucher Y, Pattier S, Cueff C, Michel M *et al*. Early structural valve deterioration of mitroflow aortic bioprosthesis: mode, incidence, and impact on outcome in a large cohort of patients. Circulation 2014;130:2012–20.
[17] Schoen FJ. Mechanisms of function and disease of natural and replacement heart valves. Annu Rev Pathol Mech Dis 2012;7:161–83.
[18] Eltchaninoff H, Durand E, Barbanti M, Abdel-Wahab M. Tavi and valve performance: update on definitions, durability, transcatheter heart valve failure modes and management. EuroIntervention 2018; 14:AB64–73.
[19] Bourguignon T, Bouquiaux-Stablo AL, Candolfi P, Mirza A, Loardi C, May MA *et al*. Very long-term outcomes of the Carpentier-Edwards Perimount valve in aortic position. Ann Thorac Surg 2015; 99:831–7.
[20] Dvir D, Bourguignon T, Otto CM, Hahn RT, Rosenhek R, Webb JG *et al*. Standardized definition of structural valve degeneration for surgical and transcatheter bioprosthetic aortic valves. Circulation 2018;137:388–99.
[21] Abbasi M, Azadani AN. Leaflet stress and strain distributions following incomplete transcatheter aortic valve expansion. J Biomech 2015;48: 3663–71.
[22] Li K, Sun W. Simulated thin pericardial bioprosthetic valve leaflet deformation under static pressure-only loading conditions: implications for percutaneous valves. Ann Biomed Eng 2010;38:2690–701.
[23] Martin C, Sun W. Comparison of transcatheter aortic valve and surgical bioprosthetic valve durability: a fatigue simulation study. J Biomech 2015;48:3026–34.
[24] Alavi SH, Groves EM, Kheradvar A. The effects of transcatheter valve crimping on pericardial leaflets. Ann Thorac Surg 2014;97:1260–6.